

AD-A150 303

RADAR INVESTIGATIONS ABOVE THE TRANS-ALASKA PIPELINE  
NEAR FAIRBANKS(U) COLD REGIONS RESEARCH AND ENGINEERING  
LAB HANOVER NH S A ARNONE ET AL. OCT 84 CRREL-84-27

1/1

UNCLASSIFIED

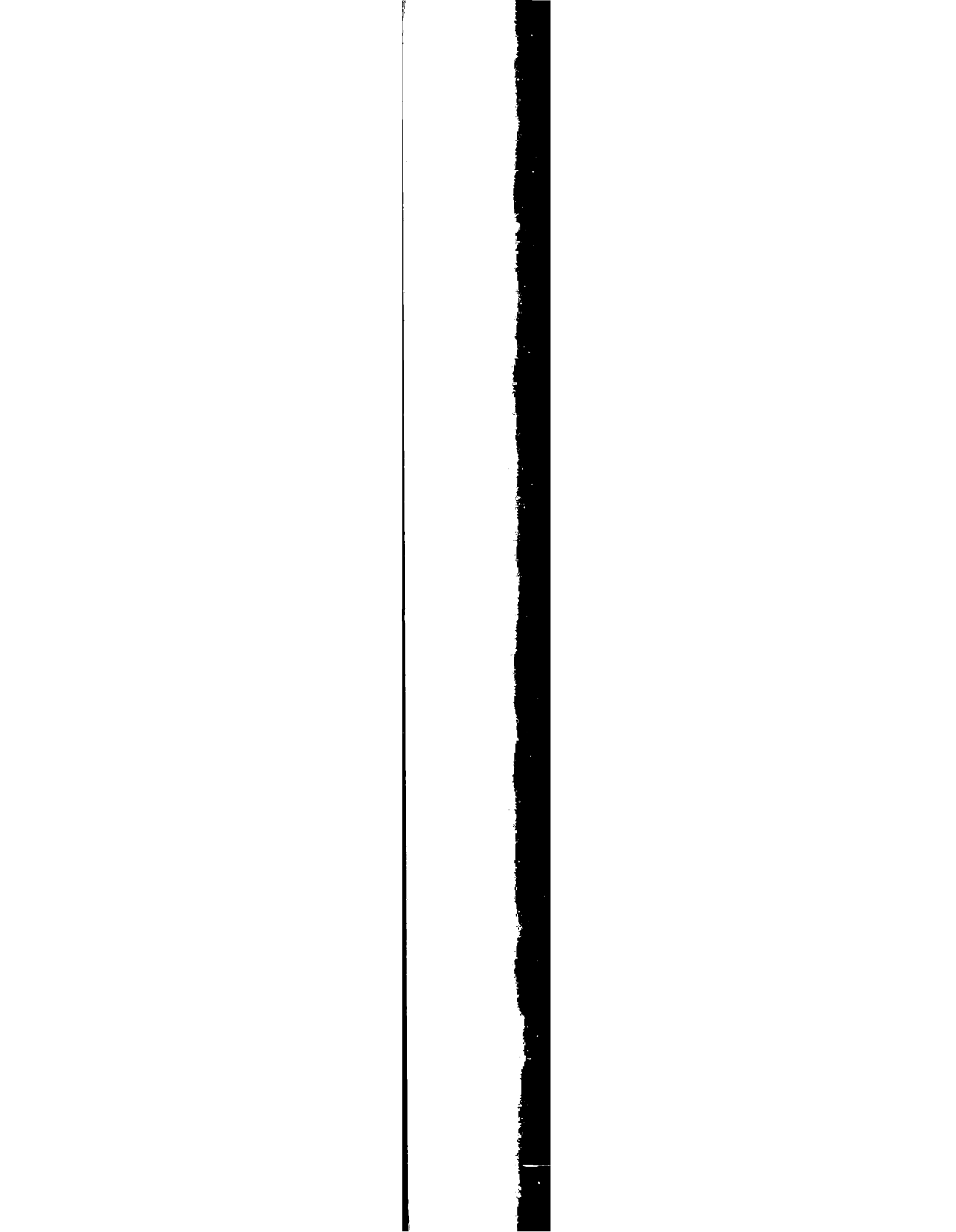
F/G 8/13

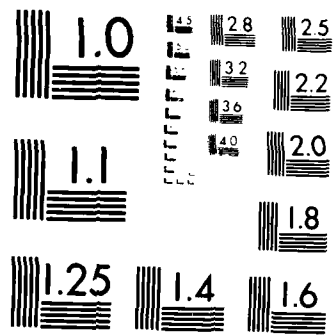
NL



END

074





MICROCOPY RESOLUTION TEST CHART  
NATIONAL BUREAU OF STANDARDS 1963-A

# CRREL

## REPORT 84-27



US Army Corps  
of Engineers

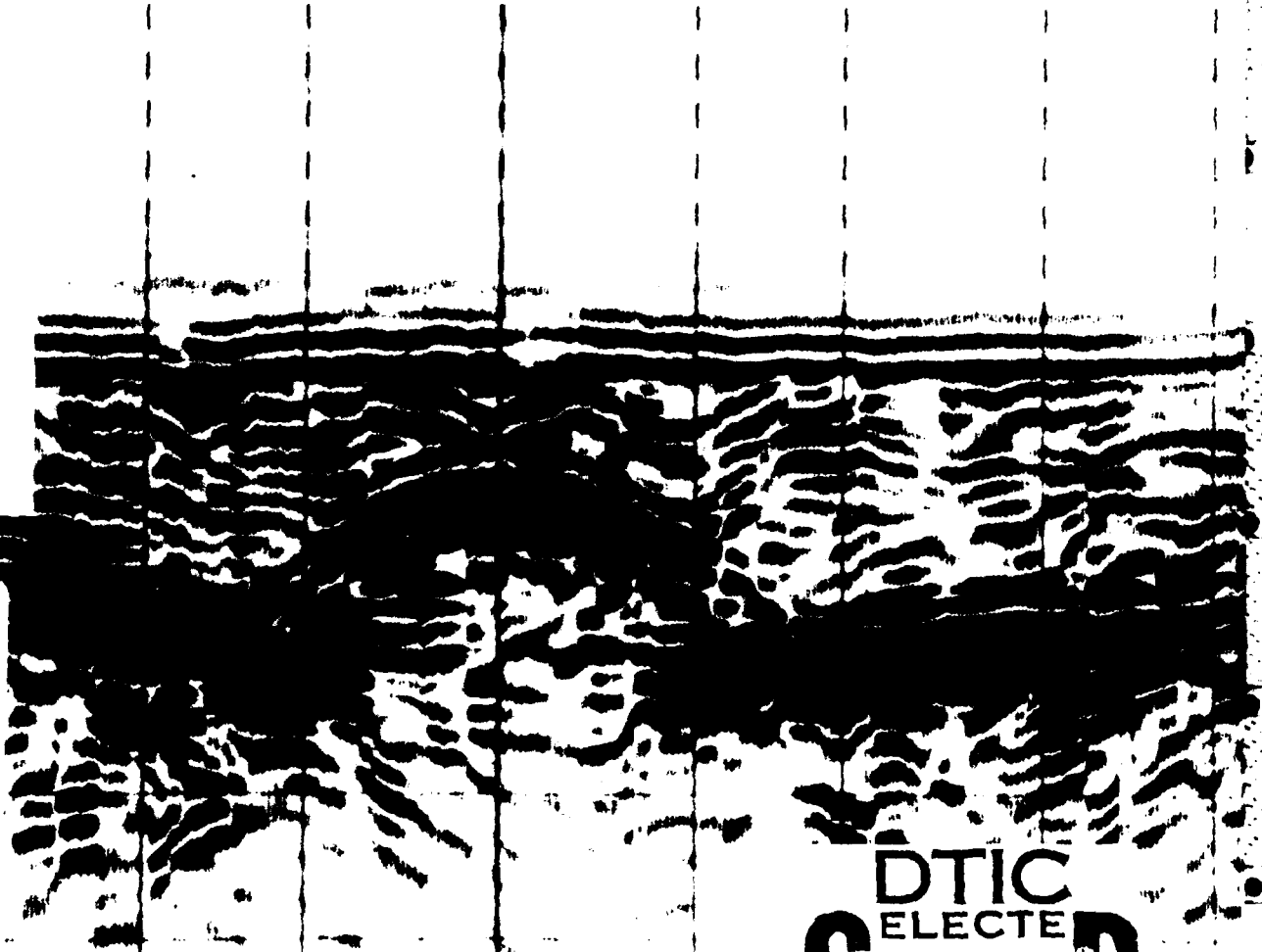
Cold Regions Research &  
Engineering Laboratory

12

### *Radar investigations above the trans-Alaska pipeline near Fairbanks*

AD-A150 303

DTIC FILE COPY



**DISTRIBUTION STATEMENT A**  
Approved for public release  
Distribution Unlimited

DTIC  
ELECTE  
FEB 12 1985  
S B

85 01 28 129

*Cover: Radar profile over section of Alyeska pipeline buried 1.93 m in gravel near Fairbanks, Alaska.*

# CRREL Report 84-27

October 1984



## *Radar investigations above the trans-Alaska pipeline near Fairbanks*

Steven A. Arcone and Allan J. Delaney

Unclassified

SECURITY CLASSIFICATION OF THIS PAGE (When Data Entered)

REPORT DOCUMENTATION PAGE		READ INSTRUCTIONS BEFORE COMPLETING FORM
1. REPORT NUMBER CRREL Report 84-27	2. GOVT ACCESSION NO. AD-A156 303	3. RECIPIENT'S CATALOG NUMBER
4. TITLE (and Subtitle) RADAR INVESTIGATIONS ABOVE THE TRANS-ALASKA PIPELINE NEAR FAIRBANKS		5. TYPE OF REPORT & PERIOD COVERED
		6. PERFORMING ORG. REPORT NUMBER
7. AUTHOR(s) Steven A. Arcone and Allan J. Delaney		8. CONTRACT OR GRANT NUMBER(s)
9. PERFORMING ORGANIZATION NAME AND ADDRESS U.S. Army Cold Regions Research and Engineering Laboratory Hanover, New Hampshire 03755		10. PROGRAM ELEMENT, PROJECT, TASK AREA & WORK UNIT NUMBERS DA Project 4A762730AT42 Task D, Work Unit 011
11. CONTROLLING OFFICE NAME AND ADDRESS Office of the Chief of Engineers Washington, D.C. 20314		12. REPORT DATE October 1984
		13. NUMBER OF PAGES 19
14. MONITORING AGENCY NAME & ADDRESS (if different from Controlling Office)		15. SECURITY CLASS. (of this report)  Unclassified
		15a. DECLASSIFICATION/DOWNGRADING SCHEDULE
16. DISTRIBUTION STATEMENT (of this Report)  Approved for public release; distribution is unlimited.		
17. DISTRIBUTION STATEMENT (of the abstract entered in Block 20, if different from Report)		
18. SUPPLEMENTARY NOTES		
19. KEY WORDS (Continue on reverse side if necessary and identify by block number) Pipelines Radar Trans-Alaska Pipeline		
20. ABSTRACT (Continue on reverse side if necessary and identify by block number) Radar and wide-angle reflection and refraction (WARR) profiles were obtained across three buried sections of the trans-Alaska pipeline near Fairbanks in late April 1983. A broad-band, pulsed radar operating in the VHF (very high frequency) range was used. The surficial geology at the three sites consisted of gravel (dredge tailings), silt and alluvium, respectively, and the sites were marginally frozen or completely thawed. At the gravel site the pipe (approximately 2 m deep) and an underlying water table were easily visible. There was no radar signature of the pipe at the silt site; the WARR profiles verified the high absorption of the material. The response was marginal at the alluvium site. High absorption due to thawing or marginal freezing conditions about the pipe makes radar a generally poor choice for mapping freeze-thaw boundaries but a good choice for estimating material state and moisture content.		

**PREFACE**

This report was prepared by Dr. Steven A. Arcone, Geophysicist, and Allan J. Delaney, Physical Science Technician, both of the Snow and Ice Branch, Research Division, U.S. Army Cold Regions Research and Engineering Laboratory. Funding for this research was provided by DA Project 4A762730AT42, *Design, Construction and Operations Technology for Cold Regions*; Task D, *Cold Regions Base Support: Design and Construction*; Work Unit 011, *Electromagnetic Geophysical Methods for Rapid Subsurface Exploration*. This report was technically reviewed by Donald Albert and Dr. Kenneth Jezek of CRREL.

The contents of this report are not to be used for advertising or promotional purposes. Citation of brand names does not constitute an official endorsement or approval of the use of such commercial products.

Accession for	
NTIS	<input checked="" type="checkbox"/>
DTIC	<input type="checkbox"/>
Unannounced	<input type="checkbox"/>
Justification	
Distribution/	
Availability Codes	
Dist	Avail and/or Special
A-1	



## CONTENTS

	Page
Abstract .....	i
Preface .....	ii
Introduction .....	1
Subsurface radar profiling and WARR sounding .....	1
Electrical properties of sediments .....	3
Methods .....	5
Results and discussion .....	5
Site 1: Goldstream Valley .....	5
Site 2: Chena Hot Springs Road .....	6
Site 3: Eielson Air Force Base .....	8
Conclusions .....	10
Literature cited .....	10
Appendix A. Debye-type dielectrics .....	15
Appendix B. Radar cross sections of targets .....	17

## ILLUSTRATIONS

### Figure

1. Idealized pulse returns and equivalent graphic display .....	2
2. Idealized WARR sounding for a two-layer ground .....	2
3. Behavior of $(n^*)^2$ for silt at about 35% volumetric water content .....	3
4. Typical conductivity ranges for thawed sediments .....	4
5. Variation of $\kappa'$ with volumetric water content for many unfrozen sediments at frequencies between about 0.1 and 4 GHz .....	4
6. Variation of $\kappa'$ with temperature for Fairbanks silt at 0.5 GHz .....	4
7. Radar profile across a buried section of the pipeline at site 1 .....	5
8. WARR profiles at site 1 .....	6
9. Radar profiles over the pipeline at site 2 .....	7
10. WARR profiles at site 2 .....	7
11. Radar profiles over the pipeline at site 3 .....	8
12. WARR profiles at site 3 with the receiver expanded over the the pipeline .....	9
13. WARR profiles at site 3 with the receiver expanded away from the pipeline .....	9

# RADAR INVESTIGATIONS ABOVE THE TRANS-ALASKA PIPELINE NEAR FAIRBANKS

Steven A. Arcone and Allan J. Delaney

## INTRODUCTION

Remote sensing of the freeze-thaw state and moisture content of the ground is of practical interest for pipeline surveying in Alaska. Thawing can cause mechanical instability due to settling, while freezing can cause the pipe to heave. Necessary to both these processes is an adequate moisture supply, which may slowly accumulate over time. Rain, melting snow, or moisture migration can all affect the local water table. Since soil dielectric properties in the very-high-frequency (VHF) through microwave-frequency bands correlate well with soil moisture content, it is possible that ground-penetrating VHF radar and its associated procedure of wide-angle reflection and refraction (WARR) profiling may be capable of remotely sensing the freeze-thaw state and ground moisture content.

The ability of ground-penetrating short-pulse radar to survey permafrost conditions has been investigated since the early 1970s. Bertram et al. (1972), Kovacs and Morey (1979) and Arcone et al. (1982) studied radar responses to massive ice. Annan and Davis (1976) and Davis et al. (1976) examined other permafrost features and first reported on the use of WARR profiling for determining dielectric properties. Pilon et al. (1979) and Arcone and Delaney (1982) used VHF radar to detect the top of the permafrost table and measure active-layer dielectric properties. Olhoeft (1978) presented a very thorough discussion of radar profiles over one buried section of the trans-Alaska pipeline. He interpreted his data to reveal construction fill boundaries, thaw margins and the pipe, but he did not measure dielectric properties directly.

Here we present radar profiles and WARR soundings taken over three pipeline burial sites near Fairbanks. The objective was to demonstrate the

use of dielectric values derived from WARR soundings for interpreting the radar profiles. Three areas, consisting primarily of gravel, silt and alluvium, respectively, were investigated. Information regarding burial depth and material type was obtained from the Trans-Alaska Pipeline System (TAPS) alignment sheets.

## SUBSURFACE RADAR PROFILING AND WARR SOUNDING

The radar equipment used for these investigations was manufactured by the Xadar Corporation and is similar to other commercially available systems. The advantages of this system include separate transmitting and receiving antennas, and digital recording to allow stacking of individual returns. This permits flexibility in choosing polarization plus an ability to do WARR profiles or one-way transmission studies. The basic principles and operation of the system have been extensively described elsewhere (e.g. Morey 1974, Annan and Davis 1976, Arcone et al. 1982) and will only be reviewed briefly.

The transmitting antenna radiates pulses of several nanoseconds duration at a repetition rate of 50 kHz. The pulse waveform approximates a single sinusoidal cycle with a short, oscillatory tail. The pulse spectrum is centered at about 300 MHz when transmission is through air. The antennas, which are resistively loaded dipoles, become more loaded when placed on the ground, decreasing the center of the pulse spectrum to between 100 and 200 MHz and placing the 3-db bandwidth generally between 75 and 300 MHz. We operated in an analog mode, for which the performance figure (the ratio of the transmitted power to the minimum detectable signal above random noise) of our

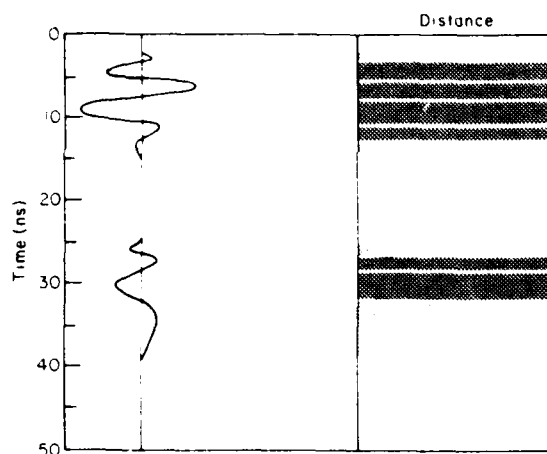


Figure 1. Idealized pulse returns and equivalent graphic display should these returns remain constant with distance.

radar is estimated at about 110 db. This figure does not include enhancement due to signal stacking (which is available on this radar in a digital mode) nor does it consider signal detection in the presence of coherent noise (unwanted signals); if it did, this figure would be considerably less.

Echos, or events, are reproduced in the audio range by sampling techniques. Time ranges from 50 to 2000 ns may be selected. A graphic display is a composite of thousands of scans (Fig. 1), with darkness proportional to the absolute value of the signal amplitude (white indicates zero amplitude). In a graphic display the horizontal axis is calibrated for antenna position and the vertical axis for time. One of several time-dependent gain functions is usually applied to the returns to compensate for the loss of amplitude with time of return.

The system is commonly used for bistatic radar profiling by towing the transmitting and receiving antennas at a fixed separation. Reflections occur at material boundaries across which contrasts in electrical properties occur. The antenna directivity, or radiation pattern, is very broad, so reflections can be received from directions other than directly beneath the antennas. Many types of events occur, but the most prevalent and easily interpretable are hyperbolic shaped from local inhomogeneities and linear as from smoothly layered bedding. If the reflectors are sloped, the slope and placement of the radar record will not necessarily be identical to that of the reflector.

Translating the radar time record into the actual subsurface geological structure requires knowl-

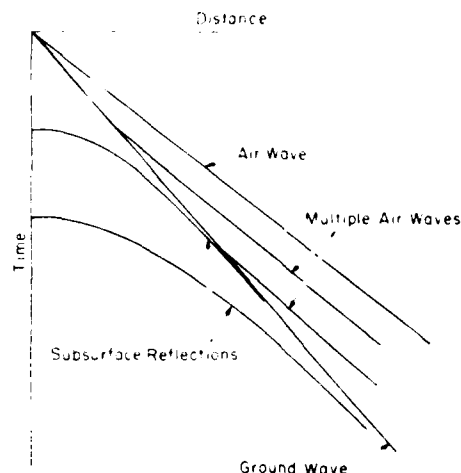


Figure 2. Idealized WARR sounding for a two-layer ground. The multiple airwaves may be caused by critical refraction of the subsurface reflections or by disturbances in the path of the ground wave.

edge of the dielectric permittivity, which determines the wave velocity within the various earth materials. This information may be obtained with a WARR sounding, which is performed by continually increasing the distance between the antennas. An idealized WARR sounding is illustrated in Figure 2 for a two-layer ground. As the antennas are separated, subsurface reflections appear; these are then analyzed for their time-distance slopes and time-axis intercepts to determine dielectric properties. The slope of the time-distance curve for the ground wave can be converted to a dielectric constant, but this wave attenuates as the square of the inverse distance, so the asymptotic slope of the first reflection will often dominate the ground wave after several meters. If the layer thickness is comparable to an in-situ wavelength of the dominant pulse frequency, waveguide multimoding and dispersion will make dielectric interpretation very difficult.

Dielectric interpretation of deeper layers is theoretically possible but rarely accomplished. However, if the dielectric constant of the lower layer  $\epsilon_2'$  is less than that of the top layer  $\epsilon_1'$ , then a refraction event may occur along the layer interface. This event will continually propagate to the surface, and its time-distance slope will allow  $\epsilon_2'$  to be evaluated.

In this report we measured the time-distance slope of the ground wave along the leading edge of the events and not along the more obvious phase fronts (the thin white lines in the graphic display are  $0^\circ$  phase fronts). This practice gives the correct

dielectric constant when dispersion occurs due only to d.c. ground conductivity (Arcone 1981).

### ELECTRICAL PROPERTIES OF SEDIMENTS

The electrical properties of interest for sediments in the VHF range are the dielectric permittivity and the electrical conductivity. Magnetic permeability is of no concern unless there is an appreciable amount of iron present. The dielectric permittivity and the conductivity together determine the complex index of refraction  $n^*$ :

$$n^* = \left[ \kappa' - i \left( \kappa'' + \frac{\sigma}{2\pi f \epsilon_0} \right) \right]^{1/2} \quad (1)$$

where  $\kappa', \kappa''$  = real and imaginary parts of the relative, complex dielectric permittivity, respectively

$$i = \sqrt{-1}$$

$f$  = frequency (Hz)

$\epsilon_0$  = absolute permittivity of free space ( $8.85 \times 10^{-12}$  F/m)

$\sigma$  = conductivity (S/m).

A harmonic time excitation  $t$  is assumed to be proportional to  $e^{i2\pi ft}$ . The real part  $\kappa'$  is generally referred to as the dielectric constant, and the total

imaginary part as the loss factor LF when  $\kappa' \gg$  LF. LF becomes important in the ultra-high-frequency (UHF) through microwave-frequency range for wet materials. Both  $\kappa'$  and LF are usually frequency dependent over this bandwidth.

The loss tangent  $\tan \delta$  is defined as

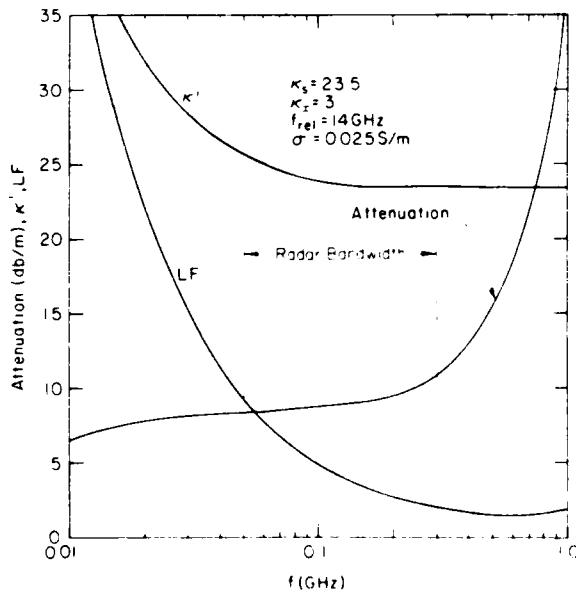
$$\tan \delta = \frac{\kappa'' + \sigma/2\pi f \epsilon_0}{\kappa'} \quad (2)$$

and is a useful number for describing materials. Insulators generally have a  $\tan \delta$  less than  $10^{-4}$  and conductors have a  $\tan \delta$  greater than 1.0. The attenuation in decibels per meter may then be found from the formula

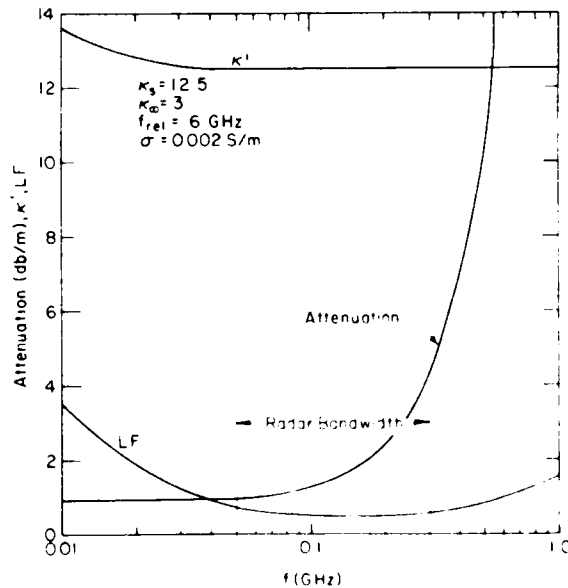
$$\text{Atten} = 8.68 \frac{2\pi f}{c} \left\{ \frac{\kappa'}{2} (1 + \sqrt{1 + \tan^2 \delta}) \right\}^{1/2} \quad (3)$$

where  $c$  is the velocity of light in free space. Equation 3 shows that attenuation increases with increasing frequency.

Figure 3 illustrates the typical behavior of  $(n^*)^2$  and the attenuation function for thawed and frozen wet silt. The curves are modeled after field and laboratory data of Arcone et al. (1978) and Delaney and Arcone (1984), which showed that thawed silt behaves like a Debye-type dielectric, the parameters of which are discussed in Appendix A. In both cases  $\kappa'$  varies little throughout the



a. Thawed.



b. Frozen ( $-2^\circ\text{C}$ ).

Figure 3. Behavior of  $(n^*)^2$  for silt at about 35% volumetric water content.  $\kappa'$  and LF are dimensionless. The dielectric parameters are discussed in Appendix A.

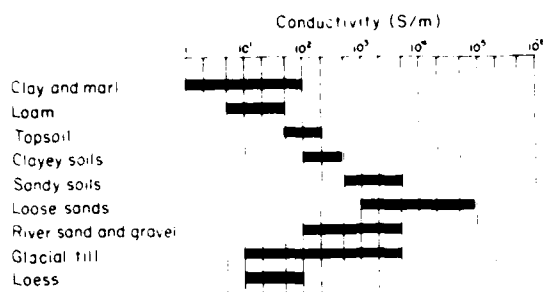


Figure 4. Typical conductivity ranges for thawed sediments.

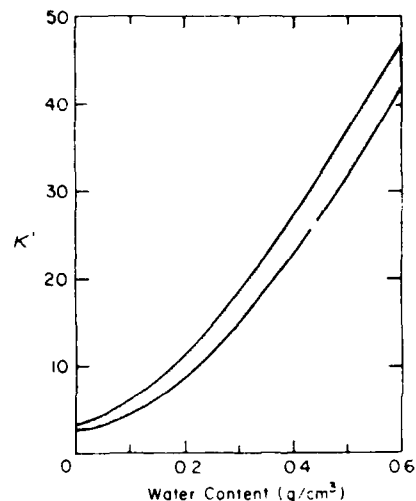


Figure 5. Variation of  $\kappa'$  with volumetric water content for many unfrozen sediments at frequencies between about 0.1 and 4 GHz. (After Topp et al. 1983.)

radar bandwidth and losses are due mainly to conductive processes. Attenuation is severe at all frequencies for the thawed case but is low for the frozen case. The rapid increase in attenuation above 0.3 GHz demonstrates why the radar bandwidth shown is a good compromise between resolution and attenuation. At much lower temperatures or very dry conditions, attenuation can be so low that higher frequencies may be used. In this case, scattering from subsurface inhomogeneities or radiated power may be a limiting factor.

Figure 4 lists some typical conductivity ranges

for thawed sediments. The range is determined mainly by the water content. Values for frozen silty, sandy or gravelly soils range from about  $3 \times 10^{-3}$  to less than  $10^{-4}$  S/m as ice content increases. Figure 5 shows the variation of  $\kappa'$  with water content for many unfrozen soils at frequencies between about 0.1 and 4 GHz. Below about 1 GHz these values are generally constant for any particular frozen or unfrozen soil.

When temperature decreases,  $\kappa'$  drops dramatically at about  $-1.5^\circ\text{C}$  for unsaturated soils, as demonstrated in Figure 6 for Fairbanks silt. This

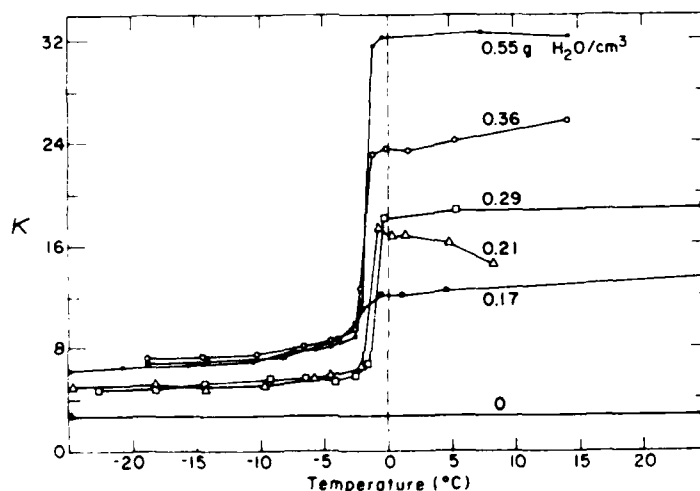


Figure 6. Variation of  $\kappa'$  with temperature for Fairbanks silt at 0.5 GHz. (After Delaney and Arcone 1982.)

occurs below 0°C because of the depressed freezing point of the free water that is within pores or adsorbed to particle surfaces. Generally, in the radar bandwidth neither  $\sigma$  nor  $\kappa''$  allows  $\tan\delta$  to exceed 0.01 below -5°C, so the dielectric values are predominantly real and vary from about 4 to 7.

## METHODS

The three sites were surveyed in late April 1983. The radar antennas were separated by 1.5 m for profiling, and the polarization was parallel with the pipe axis. Profiles and soundings were perpendicular to the pipe. The WARR soundings were taken with one antenna fixed while the other was moved. In all cases the position directly above the pipe center was determined from survey stakes or from points where the pipeline emerged from the ground. The pipeline diameter is 1.22 m.

The time scale on all records is 19.2 ns between horizontal grid lines. The variation in the interval markings is due to variations in the position of the 0-ns reference. The separation between the antennas increases the propagation distance from the surface to the pipe; this separation has been accounted for in all dielectric calculations based on profile data. The time of return can be determined to within only 1 ns. Therefore, the accuracy of dielectric constant calculations based on echo time of return increases with observation time. The same is true for dielectric constant calculations based on WARR time-distance curves.

## RESULTS AND DISCUSSION

### Site 1: Goldstream Valley

This section is located in the Goldstream valley near the old Steese Highway between Fairbanks and Fox (TAPS alignment sheet 61). The material type is a sandy, coarse gravel with some silt (dredge tailings) and is sporadically frozen. The pipeline was buried but not refrigerated at this site. The surface of a large pond within 50 m of the pipe stood 1.8 m below the ground surface above the pipe and is assumed to be the depth of the water table. The top of the pipe was 1.93 m deep, as measured in a frost heave tube.

Figure 7 shows the radar profile across the pipe. The earliest return is the direct air coupling between the antennas; this return remains at a constant time delay throughout the profile. The next return (the first dark band) is the direct ground coupling between the antennas. The time of arrival (TOA) of this event is slightly greater over the pipe than at the ends of the profile, indicating a higher dielectric constant at the surface above the pipe. The next dark band through the entire record may be the water table, which intersects the hyperbolic signature of the pipe. However, this interpretation is debatable because the depth calculated using the TOA and the dielectric constant computed from the WARR profile (discussed below) is greater than the nearby pond surface.

The TOA of the return from the top of the pipe is 35 ns. The pipe depth is 1.93 m, so the average dielectric constant above the pipe is 6.4 ( $\pm 0.4$ ). The WARR profiles (Fig. 8) expand over the pipe

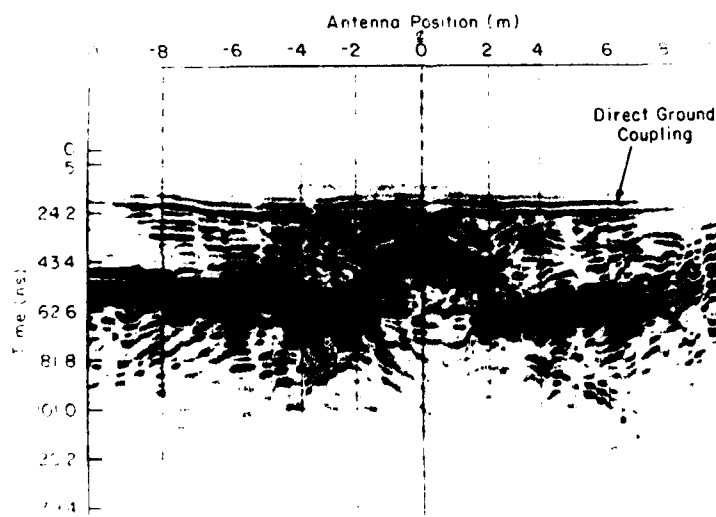
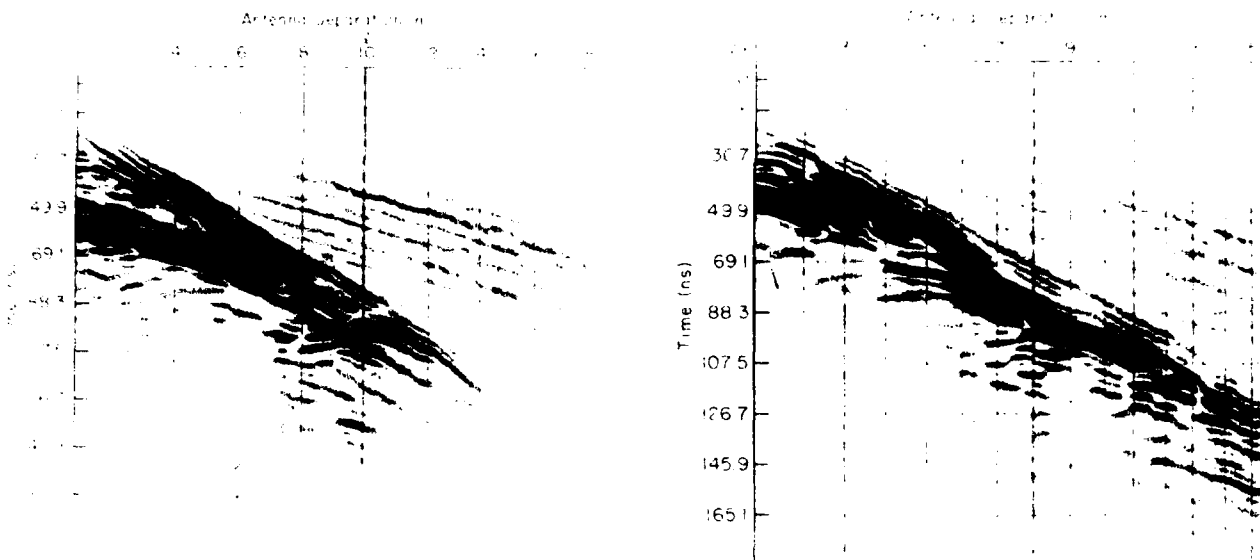


Figure 7. Radar profile across a buried section of the pipeline at site 1.



a. First profile. The center line symbol indicates the center of the pipe over which the receiver was expanded.

b. Second profile. The receiver was expanded away from the pipe.

Figure 8. WARR profiles at site 1.

and to one side of the pipe and both give a  $\kappa'$  value of 5.1 ( $\pm 0.1$ ). These values are characteristic of either very low moisture content or extremely cold conditions. As ground temperatures are no lower than  $-2^\circ\text{C}$  within 4 or 5 m of the surface throughout the region, the former interpretation is correct: the WARR profiles are showing drier conditions away from the pipe axis. The surface values of  $\kappa'$  derived from the TOA of the directly coupled ground waves are 10.2 above the pipe and between 5.8 and 8.4 beyond 8 m from either side of the pipe (all values approximately  $\pm 1.2$ ). Therefore, the gravel in this area is probably fairly dry and frozen, with slightly warmer conditions above the pipe and along the surface.

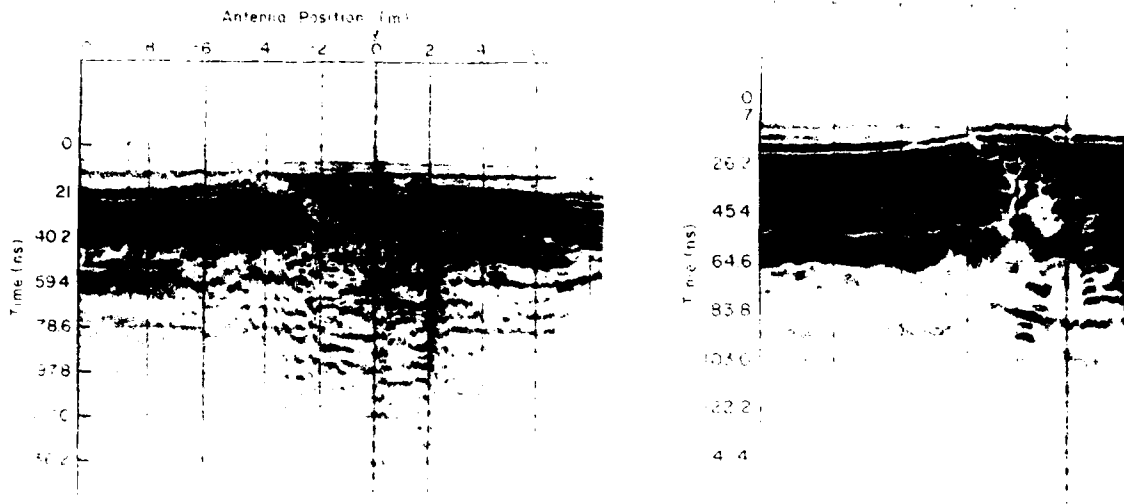
We are cautious about interpreting the strong linear reflector as the water table because the minimum time delay (45 ns at 10 m) and the dielectric constant (5.1) give a depth of about 3.0 m, whereas the nearby pond surface was only 1.80 m below the ground surface above the pipe. However, the radar reflection does elevate in time with distance from the pipe, so it may ultimately merge with the pond elevation. The water table may dip below the pipeline due to a less permeable fill around the pipe. It is unlikely that this reflector could be the gravel/bedrock interface, because the tailings are deep in this area.

#### Site 2: Chena Hot Springs Road

This section is located at the buried pipeline crossing north of the Chena Hot Springs road (TAPS alignment sheet 60). The crossing occurs at a ridgetop, and the burial continues for over 50 m under a small clearing on the north side of the road, allowing easy access for radar profiling. The material type is classified by P  w   et al. (1966) as unfrozen loess. The alignment sheet shows that the top of the pipe is 3 m deep.

Two radar profiles over the pipe are shown in Figure 9. The profile in Figure 9a was performed with the antenna supplied by the manufacturer; this antenna was also used at the gravel site. The center frequency of the direct ground coupling is approximately 140 MHz, as measured from the uppermost set of heavy, dark bands. No signature from the pipe (at the 0-m position) is visible on the record. The TOA of the direct coupling decreases at the  $-2$  m position, indicating better surface drainage. The TOA of the direct ground coupling at the ends of the profile gives a  $\kappa'$  of approximately 12.3 ( $\pm 1.4$ ), while nearer the pipe the TOA gives a  $\kappa'$  of approximately 4.8.

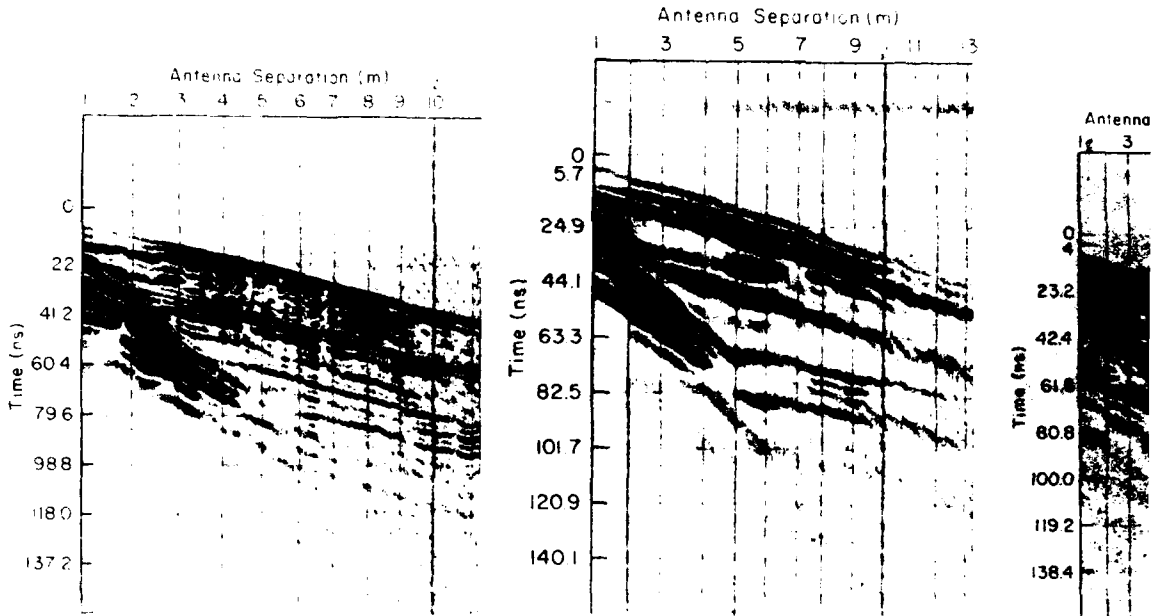
Figure 9b gives a radar profile using antennas we made in hopes of increasing penetration and detecting the pipe. This antenna had a much lower center frequency of approximately 80 MHz. Again



a. 140 MHz.

b. 80 MHz.

Figure 9. Radar profiles over the pipeline at site 2. The disturbance between 0 and 2 m is a resonance related conditions.



a. 110 MHz.

b. 80 MHz; receiver expanded over the pipeline.

c. 80 MHz; receiver away from the pipeline.

Figure 10. WARR profiles at site 2.

there is no pipe signature, and there are similar decreases in the TOA of the direct ground couplings at the ends of the profile. This lack of response implies wet conditions and severe attenuation over the 6-m propagation path.

WARR profiles are presented in Figure 10. Fig-

ure 10a is with the higher-frequency antenna and the wave becomes a composite of ground wave and a reflection from a buried reflector, perhaps the bottom of the pipe. The amplitude is severely att

more than 5 m of separation; the small portion available gives a  $\kappa'$  of about  $10.5 (\pm 0.9)$ . Figures 10b and c give the 80-MHz response taken in two directions over the pipe. In Figure 10b the transmitter was fixed 10 m away from the pipe and the receiver was expanded towards the pipe; in Figure 10c the transmitter was fixed above the pipe and the receiver was expanded away from the pipe. In 10b  $\kappa'$  is approximately  $15.2 (\pm 1.2)$ , and the ground wave is gone by 5 m; in 10c the attenuation is so great that there is only a slight suggestion of a ground wave within the first 2 m, and  $\kappa'$  cannot be determined.

The WARR profiles verify the highly absorptive nature of this overburden. Figure 5 suggests that the water content by volume is about 25-30% when  $\kappa'$  is approximately 15.2; this value is similar to dielectric values measured in the Fairbanks area, where resistivity was about  $40 \Omega\text{-m}$  for the same material (Sellmann et al. 1983). The measurements of Delaney and Arcone (1982) on Fairbanks silt suggest a volumetric water content of 20-25% at temperatures just above  $0^\circ\text{C}$ . The dipolar contribution to  $\kappa''$  at these water contents for 100 MHz is very small, so I.F. is determined by conductivity effects. At a resistivity value of  $40 \Omega\text{-m}$  for thawed silt at a  $\kappa'$  of 15,  $LF = 4.5$ , giving an attenuation rate of  $10.4 \text{ db/m}$ , or about  $62 \text{ db}$  for the 6-m propagation distance.

This loss of  $62 \text{ db}$  plus losses due to beam spreading (approximately  $16 \text{ db}$ ) and due to the effective cross-sectional area of the pipe (approximately  $6 \text{ db}$ ; Appendix B) gives an estimated total loss of  $84 \text{ db}$ , which should have provided only a marginal response under the ideal conditions of no background noise. As is obvious from Figure 9, however, there are strong near-surface reflections that further decrease the depth of penetration and put the desired pipe response far below the level of the background geologic (coherent) noise.

### Site 3: Eielson Air Force Base

This conventionally buried section is located approximately 32 km south of Fairbanks (TAPS alignment sheet 57). The area is within the Tanana floodplain, and the material type is alluvium. The placement of the pipe axis was determined to within 1 m using survey marks; the pipe did not surface within view. As best we could determine from the alignment sheets, the depth of the pipe at this sandy site was between 1.1 and 1.4 m.

Figure 11 shows the profiles made with the Xadar antenna (140 MHz) and our antenna (80 MHz). A possible hyperbolic response can be seen at about 40 ns in Figure 11a just to the right of the

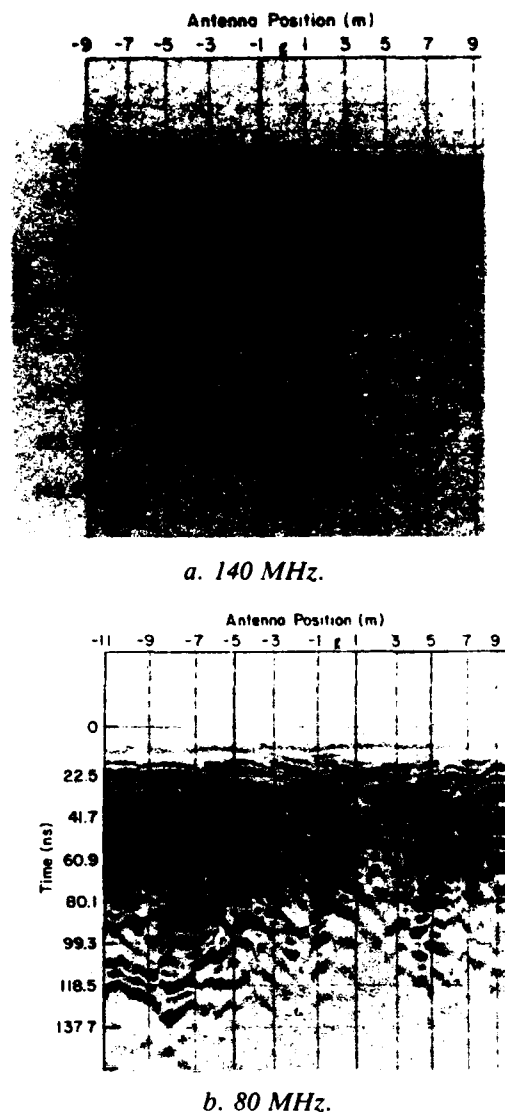
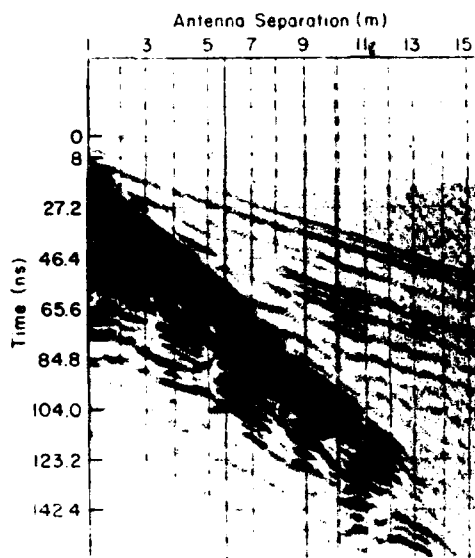


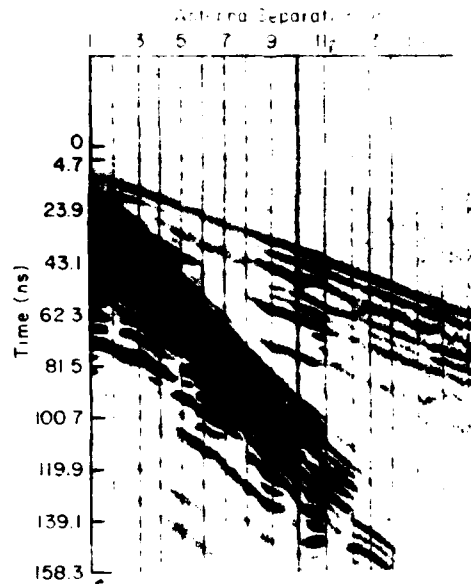
Figure 11. Radar profiles over the pipeline at site 3.

assumed centerline. Another possible hyperbolic response is visible at about 45 ns in Figure 11b at the same position, but it is not unique within the record. Both profiles reveal many other strong reflectors within the backfill, obscuring the pipe response.

The WARR profiles of Figures 12a (140 MHz) and 12b (80 MHz) were performed with the transmitter about 11 m off the assumed pipe axis and the receiver expanded toward the pipe. Both figures show a good ground-wave response and strong subsurface reflections. The ground waves give  $\kappa'$  values of approximately 7.7 and  $7.5 (\pm 0.2)$  for Figures 12a and b, respectively. In both figures,

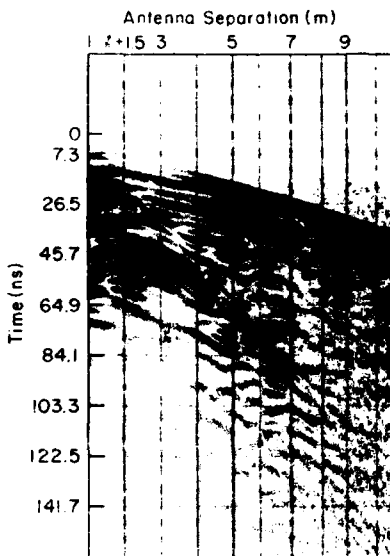


a. 140 MHz.

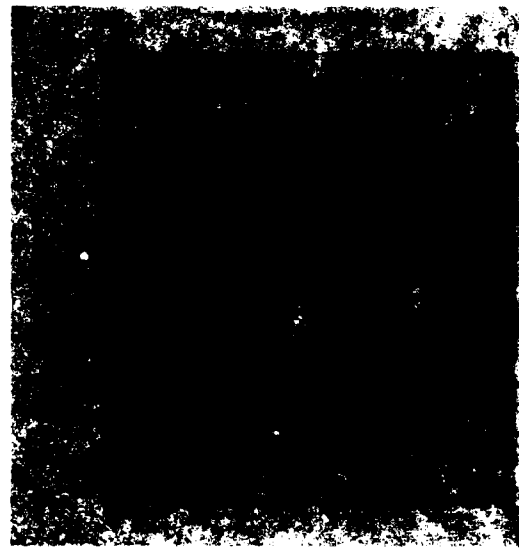


b. 80 MHz.

Figure 12. WARR profiles at site 3 with the receiver expanded over the pipeline.



a. 140 MHz.



b. 80 MHz.

Figure 13. WARR profiles at site 3 with the receiver expanded away from the pipeline.

faint hyperbolic responses can be seen centered at about 12 m. The TOAs of the peaks of these hyperbolae are both  $137 \pm 2$  ns; this is close to the theoretical value of 130 ns for an assumed straight-ray propagation path through alluvium ( $\kappa' = 7.7$ ) and trench fill ( $\kappa' = 12.1$ , discussed below) at an estimated depth of 1.2 m. Therefore,

it is assumed that these events are caused by the pipe.

The WARR profiles (Fig. 13) were performed with the transmitter situated above the pipe. The ground wave of Figure 13a gives a  $\kappa'$  estimated at between 8.5 and 12.1, as there is no easily identifiable leading edge to the ground events. The actual

ground wave disappears after the 4-m mark, and the remaining events are subsurface reflections. This is also true of Figure 13b, where the ground responses are so severely attenuated that no value of  $\kappa'$  can be estimated, indicating a highly absorptive trench fill above the pipe. Figure 13a shows an interesting response centered at 3 m that seems to be hyperbolic. The delay to the peak of this response is about 37 ns at an antenna separation of 2.5 m. If the pipe depth was 1.2 m, this delay gives a  $\kappa'$  of 10.3, which falls in the range calculated from the ground waves. Therefore, this event is most likely a pipe response.

## CONCLUSIONS

The ability of subsurface radar operating in the VHF band to detect the trans-Alaska pipeline depends mainly on ground conditions. The average depth (less than 2 m) and the size of the backscattering cross section make the pipe a sufficiently large and close target for detection when it is buried in a homogeneous dielectric (site 1). However, when the fill is a marginally frozen or thawed silt or an extremely inhomogeneous alluvium, absorption or noise can mask the returns. Since the "thawed" electrical properties of fine-grain materials occur above about  $-1.5^{\circ}\text{C}$ , it is highly unlikely that any fine-grain fill will be cold enough to sufficiently reduce conductive absorption in interior Alaska.

Generally the absorptive and inhomogeneous nature of marginally frozen or thawed ground would make pipeline or subsurface freeze-thaw boundary detection difficult at depths beyond even one meter. Therefore, short-pulse propagation would be best used for gathering dielectric information from ground-wave studies. This information, coupled with a knowledge of material type, should allow estimates of the extent of material thaw around the pipe. When the pipe is visible on the radar profile record, knowledge of the pipe depth may be used with the measured time of return to expand the WARR dielectric information.

## LITERATURE CITED

- Annan, A.P. and J.L. Davis** (1976) Impulse radar sounding in permafrost. *Radio Science*, 11 (4): 383-394.
- Arcone, S.A.** (1981) Distortion of model subsurface radar pulses in complex dielectrics. *Radio Science*, 16(5): 855-864.
- Arcone, S.A. and A.J. Delaney** (1982) Dielectric properties of thawed active layers overlying permafrost using radar at VHF. *Radio Science*, 17(3): 618-626.
- Arcone, S.A., P.V. Sellmann and A.J. Delaney** (1978) Shallow electromagnetic geophysical investigations of permafrost. In *Proceedings, Third International Conference on Permafrost, Edmonton, Alberta*, vol. 1, pp. 501-507.
- Arcone, S.A., P.V. Sellmann and A.J. Delaney** (1982) Radar detection of ice wedges in Alaska. USA Cold Regions Research and Engineering Laboratory, CRREL Report 82-43.
- Bertram, C.L., K.J. Campbell and S.S. Sandler** (1972) Locating large masses of ground ice with an impulse radar system. In *Proceedings of the Eighth International Symposium on Remote Sensing of the Environment, Ann Arbor, Michigan*, pp. 241-260.
- Davis, J.L., W.J. Scott, R.M. Morey and A.P. Annan** (1976) Impulse radar experiments on permafrost near Tuktoyaktuk, N.W.T. *Canadian Journal of Earth Sciences*, 13: 1584-1590.
- Debye, P.** (1929) *Polar Molecules*. The Chemical Catalog Co., Inc. Reprinted by Dover Publications, New York, 1945.
- Delaney, A.J. and S.A. Arcone** (1984) Dielectric measurements of frozen silt using time domain reflectometry. *Cold Regions Science and Technology*, 9: 39-46.
- Kovacs, A. and R.M. Morey** (1979) Remote detection of massive ice in permafrost along the Alyeska Pipeline and the pump station feeder gas pipeline. In *Proceedings of the American Society of Civil Engineers Specialty Conference on Pipelines in Adverse Environments, New Orleans*, vol. 1, pp. 268-280.
- Morey, R.M.** (1974) Continuous subsurface profiling by impulse radar. In *Proceedings of the Engineering Foundation Conference on Subsurface Exploration for Underground Excavation and Heavy Construction*. American Society of Civil Engineers, New York, pp. 213-232.
- Olhoeft, G.R.** (1978) Thawing of permafrost along the trans-Alaska pipeline. In *Proceedings of a Symposium on Permafrost Geophysics (No. 5)*. Technical memorandum no. 128, National Research Council, Ottawa, Canada.
- Péwé, T.L., C. Wahrhaftig and F. Weber** (1966) Geologic map of the Fairbanks Quadrangle, Alaska. U.S. Geological Survey Map I-455.
- Pilon, J.A., A.P. Annan, J.L. Davis and J.T. Gray** (1979) Comparison of thermal and radar active layer measurement techniques in the Leaf Bay area, Nouveau-Québec. *Géographique Physique et Quaternaire*, 33(3,4): 317-326 (in French).

**Sellmann, P.V., S.A. Arcone and A.J. Delaney**  
(1983) Radar profiling of buried reflectors and the  
ground water table. USA Cold Regions Research  
and Engineering Laboratory, CRREL Report  
83-11.

**Topp, G.C., J.L. Davis and A.P. Annan (1980)**  
Electromagnetic determination of soil water con-  
tent: Measurements in coaxial transmission lines.  
*Water Resources Research*, 16(3): 574-582.

## APPENDIX A. DEBYE-TYPE DIELECTRICS

Materials containing unfrozen water, whether free or bound to the material, exhibit frequency-dependent dielectric properties in the VHF through microwave-frequency range. This type of frequency dependence was first discussed by Debye (1929) and is described as a relaxation-type phenomenon. In a relaxation-type process the atomic or molecular dipoles (water molecules are permanent dipoles) fail to keep in phase with the impinging electromagnetic field within a critical frequency range, so they convert the electromagnetic energy into heat. The characteristic frequency at which this happens is known as the relaxation frequency. For liquid water at 20°C it is about 22 GHz, and at 0°C it is about 9 GHz. For water adsorbed on thawed soils it is generally between 1 and 9 GHz and may range as low as 300 MHz for frozen soils.

Mathematically the complex relative dielectric permittivity  $\kappa^*$  may be expressed as

$$\kappa^* = \kappa_\infty + \frac{\kappa_s - \kappa_\infty}{1 + if/f_{rel}} \quad (A1)$$

where  $\kappa_s$  = low-frequency (or static) dielectric constant

$\kappa_\infty$  = high-frequency (or electronic) dielectric constant

$f$  = frequency of excitation

$f_{rel}$  = relaxation frequency.

The quantities  $\kappa'$  and  $\kappa''$  discussed in the text are the real and imaginary parts of  $\kappa^*$ . The complex index of refraction  $n^* = \sqrt{\kappa^*}$ .

## APPENDIX B: RADAR CROSS SECTIONS OF TARGETS

A wealth of literature exists on the backscattering properties of targets. Solutions are readily available for the backscattered field strength from simple geometric shapes, such as spheres and cylinders, as a function of the ratio of circumference to wavelength. Since our situation deals with a broad-band pulse for which no specific solution exists, the approximate loss of power due to pipe reflection was determined experimentally as follows.

If the pulse center frequency is 110 MHz (as observed at the Chena Hot Springs site) and the dielectric constant in wet silt is about 15, the approximate in-situ dominant wavelength of the pulse is

about 70 cm. This is also approximately the outer radius of the pipeline, so the ratio of circumference to in-situ wavelength was about  $2\pi$ . Using a GSSI\* Model 101C antenna, which radiates a pulse shape similar to that of the Xadar antennas at a center wavelength of approximately 45 cm (in air), we then compared the peak signal levels of the reflections from a flat metal plate (approximately 4 m<sup>2</sup>) and a metal, cylindrical water tank (with a radius of 46 cm) held at the same distance from the antennas. The comparison showed a loss of 6 db in peak signal level and little distortion in pulse waveform.

---

\*Geophysical Survey Systems, Inc., Hudson, N.H.

A facsimile catalog card in Library of Congress MARC format is reproduced below.

Arcone, Steven A.

Radar investigations above the trans-Alaska pipeline near Fairbanks / by Steven A. Arcone and Allan J. Delaney. Hanover, N.H.: Cold Regions Research and Engineering Laboratory; Springfield, Va.: available from National Technical Information Service, 1984.

iii, 19 p., illus.; 28 cm. ( CRREL Report 84-27. )

Prepared for Office of the Chief of Engineers by Corps of Engineers, U.S. Army Cold Regions Research and Engineering Laboratory under DA Project 4A762730 AT42.

Bibliography: p. 10.

1. Pipelines. 2. Radar. 3. Trans-Alaska Pipeline. I. Delaney, Allan J. II. United States. Army. Corps of Engineers. III. Cold Regions Research and Engineering Laboratory, Hanover, N.H. IV. Series: CRREL Report 84-27.

**END**

**FILMED**

**3-85**

**DTIC**

